Modeling the lateral organization of collagen molecules in fibrils using the paracrystal concept

Jean Doucet, Fatma Briki, Aurélien Gourrier, Chantal Pichon, Laurie Gumez, Sabine Bensamoun, Jean-François Sadoc

Modelling the lateral organization of collagen molecules in fibrils using the paracrystal concept

Jean Doucet[1], Fatma Briki[1], Aurélien Gourrier[1,2], Chantal Pichon[3], Laurie Gumez[4], Sabine Bensamoun[4], Jean-François Sadoc[1]

[1] Laboratoire de Physique des Solides, UMR8502 Université Paris-Sud 11 F-91405 Orsay

[2] European Synchrotron Radiation Facility, F-38043 Grenoble

[3] Centre de Biophysique Moléculaire CNRS UPR 4301, F-45100 Orléans

[4] Laboratoire Biomécanique et Bioingénierie, UMR CNRS 6600, UTC, F-60205 Compiègne

corresponding author

Jean Doucet

Laboratoire de Physique des Solides, Bât. 510,

Université Paris-Sud 11

F-91405 Orsay (France)

email : doucet@lps.u-psud.fr

tel: +33 (0)1 69 15 50 23

fax : +33 (0)1 69 15 60 86

Abstract

The dense phases formed by fibre-shaped molecules are usually characterized by the organization into parallel rods packed into a hexagonal or pseudo-hexagonal lateral network. This is the case for the collagen triple helices inside fibrils. Their fine pseudo-hexagonal organization has been recently deduced from X-ray diffraction experiments carried out on highly crystallised fibres which are obtained by immersing the freshly extracted fibres into a salt-controled medium. However the scattering patterns display generally additional diffuse features which are characteristc of a poorly defined lateral order, similar to those we observed in the scattering patterns of freshly extracted and untreated fibres. Only few studies have analysed and modelled the lateral packing of collagen triple helices when the structure is disordered. Some authors have used the concept of short range order but this model does not contain any echo of a hexagonal order. In order to retain the hexagonal symmetry, we use here the analytical paracrystal approach, which leads to a good agreement with experiment in the medium-angle region. This modelling method is quite sensitive to the degree of disorder and to the average inter-object distance. One clear and unexpected result is that the shift of peak positions can arise from a change in the degree of order without any change of the distances. This underlines the importance of evaluating the degree of order before attributing a shift in peak position to a change in the unit cell. This modelling method can be used for all rod-shaped molecules.

Keywords : collagen fibril - X-ray scattering - paracrystal - lateral order

1. Introduction

The dense phases formed by fibre-shaped molecules in natural or synthetic materials are usually characterized by the organization into parallel rods in order to optimize their compactness and physical properties at the nano- and mesoscopic scales. This basic structure is often influenced by the helical nature of the molecule giving rise to an approximately circular cross-section. Chirality also results in a torsion between the molecules, as observed in more diluted liquid-crystalline phases [1] [2]. However, since a maximum of compactness and a uniform torsion are not compatible, strain appear in these geometrically frustrated systems. The strains are generally hindered to a non-negligible extent in dense materials, resulting in structural disorder. The degree of structural disorder can range from a total lack of long-range order to very complex crystalline or even quasi-periodical phases, which nature is very sensitive to the physical parameters and chemical impurities.

Collagen is one the most abundant fibrous protein in human tissues. It is formed by three left-handed α-chains folded into right-handed triple helix molecules with a large length to width ratio (about 200). For most collagen types, the triple-helices assemble into tightly packed super-coiled fibrils. The number of collagen molecules in a fibril cross-section varies from about one hundred up to more than one thousand for the largest fibrils. Their fine lateral organization is still an important matter of debate since this plays a crucial role in the biomechanical properties of many organs (e.g. skin, cornea, bones, teeth). The X-ray scattering patterns are somewhat confusing with this respect since they often show a mixture of Bragg spots, indicative of a long-range crystalline phase, and of diffuse scattering characteristic of a short-range order only. Nevertheless, most authors agree on a description by a pseudo-hexagonal 2D-array [3]. The situation is further complicated by the high sensitivity of the collagen structure to many parameters such as hygrometry, salt conditions, pH, origin and type of tissues, etc.

Due to the large number of parameters that can affect the collagen structure, and thus its packing behaviour in the fibrils, modelling studies are therefore crucial to assess the influence of variables that are difficult to access experimentally. A first approach to describe a structural disorder retaining a local order consists to start from a perfect periodical crystalline order, and then to introduce topological defects (dislocations, disclinations) which break the positional and/or orientational orders [4]. The parameters of the model are obtained after a series of

fitting cycles by comparison between the experimental scattering data and the simulated ones. Another way is to simulate the structure with the molecules in a dynamic state, but it is computationaly very heavy and difficult with such large supramolecular assemblies.

An interesting alternative approach has been developed for liquids by Percus and Yevich [5] which allows the possibility to relate a possible interaction to the structure factor. This method was proposed in 1976 by Woodhead-Galway and Machin [6] to derive a collagen model using rigid cylinders interacting *via* a hard core potential.
In a previous study, we have developed an approach similar to that of Woodhead-Galway and Machin to study the organization of the keratin intermediate filaments in hair cells [7]. However, the relative positions of molecules were not derived from a hard core potential but from a model of short-range crystalline order using the paracrystal concept [8]. For a paracrystal model, the array is distorted in such a way that the the unit cells retain a parallelogram shape. Such approximation leads to an analytical expression of the relative positions of molecules in the case of rectangular arrays. We have further extended its application field to the case of the hexagonal array [9]. The implementation of this model is relatively straightforward owing to its analytical nature and to to the fact that the fine details of the structure needn't be considered. Additionally, the model depends on a limited set of parameters: the diameter of the molecular cross-sections, the average unit cell length and the degree of disorder of the paracrystalline network.

The purpose of the present study is to use the same modelling approach to analyse the lateral organization of the collagen molecules across the fibril sections in the native state of the tissue, i.e. when not crystallized. More specifically, the aim is to characterize the structure giving rise to the diffuse features which appear in the X-ray scattering patterns produced by fibres extracted from the tissue without further treatment. These features are also generally present in patterns of fibres maintained in a controlled salt and hydration environment, superimposed to sharp diffraction reflections from crystallized zones. The traditional approaches of crystallography of proteins usually adopted to obtain a high resolution structure of the crystallized zones from the Bragg reflections [10] are therefore out of scope of the present study. Let us emphasize that our study is limited to the transverse equatorial organization of the collagen molecules, thus excluding any analysis of the correlations between longitudinal and transverse structures.

2. Materials and methods

2.1 samples: fibres from mouse tail

Eight three-month old female C57Black/6 wild-type (WT) mice were used. The mice were sacrificed with CO_2 and tails were amputated close to the body attachment. Five tails were frozen and stored at –80°C and three tails were directly used for experimentation to establish the impact of cold-storage on tendon structure. Under a stereomicroscope, approximately 2-3 tendon fibres were extracted from each tail. Then, single tendon fibres (N_{frozen} = 9, N_{fresh} = 4) were inserted right away into a glass capillary (diameter = 0.7mm) which was immediately sealed and placed vertically in the X-ray beam. The preparation time could vary between 30 s and 2 minutes, inducing different degrees of humidity for the tendon fibre.

2.2 X-ray scattering data collection

The experiments were performed at the European Synchrotron Radiation Facility (Grenoble, France) on the microfocus beamline ID13 [11]. The high intensity monochromatic beam (wavelength λ = 0.9621 Å), obtained from an in-vacuum undulator and a Si(111) double-crystal monochromator, was focused with an ellipsoidal mirror (focal spot 20(h)x40(v) μm^2) and a size-limited down to a 2 μm diameter section by a Kirpatrick-Baez optics. A two-pieces guard aperture (Pb, about 10 μm square aperture) reduced diffuse scattering from the collimator exit. Samples were mounted with the fibre axis vertical, perpendicularly to the X-ray beam, on a computer-controlled gantry coupled with a microscope allowing to adjust the position of the sample with a resolution close to 0.1 μm.

The experiments were carried out at a sample-detector distance of 344.5 mm, which was calibrated using silver behenate (first order spacing 58.38 Å). Using a ~200 μm diameter beam-stop, two-dimensional X-ray scattering patterns were recorded from 0.005 to 0.4 $Å^{-1}$ on a MAR-CCD camera (16 bit readout; 130 mm entrance window; 2048 x 2048 pixels; pixel size of 78.94 x 78.94 μm^2).

The data collection procedure consisted in a series of transverse scans (perpendicular to the fibres), at least three for each sample, with a step size between 2 and 4 μm. Time exposure for recording a pattern was 2 s. No radiation damage effect was detected on the scattering pattern for this exposure time.

Data analysis was carried out using the equatorial profiles obtained by azimuthal integration of the intensity within a ± 20° angular range.

2.3 X-ray scattering modelling

The modelling method based on the paracrystal concept was developed a few years ago for keratin fibres [7]. Briefly, the scattered intensity is proportional to the square modulus of the electronic density Fourier Transform. The intrafibrillar electronic density can be described as triple helices located on the set of points defined by the position function. In the present study, we will only consider the equatorial modelling, *i.e.* a two-dimensional problem. The electronic density $\rho(\boldsymbol{r})$ projected onto the fibril cross-section is equal to the convolution product of the electronic density projection of a triple helix $\rho_m(\boldsymbol{r})$ with the position function $p(\boldsymbol{r})$:

$$\rho(\boldsymbol{r}) = \rho_m(\boldsymbol{r}) * p(\boldsymbol{r}) \quad (1)$$

The scattered amplitude $A(\boldsymbol{S})$ is proportional to the Fourier transform of $\rho(\boldsymbol{r})$

$$A(\boldsymbol{S}) = F_m(\boldsymbol{S}).P(\boldsymbol{S}) \quad (2)$$

with $F_m(\boldsymbol{S})$ and $P(\boldsymbol{S})$ the Fourier transform of $\rho_m(\boldsymbol{r})$ and $p(\boldsymbol{r})$ respectively, and $\boldsymbol{S}$ the scattering vector.

The general expression of the scattered intensity (outside $\boldsymbol{S}=0$) is thus proportional to:

$$I(\boldsymbol{S}) = |F_m(\boldsymbol{S})|^2.|P(\boldsymbol{S})|^2 \quad (3)$$

It is more convenient to handle distribution functions rather than position functions. Besides, the distribution function $z(\boldsymbol{S})$ gives the probability to find an object at position $\boldsymbol{r}$. The interference function $Z(\boldsymbol{S})$, which is the Fourier transform of $z(\boldsymbol{r})$, is equal to $|P(\boldsymbol{S})|^2$. The final expression for the scattered intensity becomes :

$$I(\boldsymbol{S}) = |F_m(\boldsymbol{S})|^2. Z(\boldsymbol{S}) \quad (4)$$

The distribution function $z(\boldsymbol{r})$ of microfibrils sections in the equatorial plane has to reflect the fact that the crystalline order only extends at short-range. R. Hoseman in years 1950 has introduced the paracrystal concept [8], a special case of short range order obtained by deforming an orthorhombic lattice in such a way that the unit cells all retain a parallelogram shape. The advantage of the paracrystal description lies in the fact that $Z(\boldsymbol{S})$ is an analytical function.

It has been shown that $Z(\boldsymbol{S})$ is still analytical in the case of an hexagonal lattice ($\boldsymbol{a}$,$\boldsymbol{b}$) when introducing a third distribution function between first neighbours along the -($\boldsymbol{a}$+$\boldsymbol{b}$) axis ($\boldsymbol{c}$-axis

hereafter). The distribution for the ***c***-axis is identical to those for ***a*** and ***b***-axes, in order not to break the sixfold symmetry [9]. In the case of a Gaussian distribution of the unit cell length with a standard deviation, the final expression of the interference function becomes:

$$Z(S) = 2\,\mathrm{Re}\left(\frac{H_1^a}{1-H_1^a}\frac{\overline{H_1^b}}{1-\overline{H_1^b}}\right) + 2\,\mathrm{Re}\left(\frac{H_1^a}{1-H_1^a}\frac{H_1^c}{1-H_1^c}\right) + 2\,\mathrm{Re}\left(\frac{H_1^b}{1-H_1^b}\frac{H_1^c}{1-H_1^c}\right) + 2\,\mathrm{Re}\left(\frac{H_1^a}{1-H_1^a}\right) + 2\,\mathrm{Re}\left(\frac{H_1^b}{1-H_1^b}\right) + 2\,\mathrm{Re}\left(\frac{H_1^c}{1-H_1^c}\right) + 1 \qquad (5)$$

with $H_1^j = \exp(-4\pi^2\sigma^2 \boldsymbol{S}^2/3).\exp(-2i\pi \boldsymbol{S}.\boldsymbol{j})$, ***j*** = ***a***, ***b*** or ***c***, and Re means the real part.

The interference function Z(***S***) displays series of maxima centered on the reciprocal nodes; their width increases with indexes and they finally disappear as rapidly as the standard deviations are large. Finally, an integration of Z(***S***) over 360° in the equatorial plane is necessary to take into account all orientations of hexagonal axes in the case of a random orientation of the "crystallites", which is a common feature of the packing of fibres in tissues. Therefore, the modelling only depends on three parameters: the average distance between molecules (which is directly related to the unit cell length), its standard deviation and the Fourier transform of the electronic molecular projection.

3. Results

3.1 Experimental X-ray scattering patterns

Figure 1 shows the inner zone of three X-ray diffraction patterns. They correspond to different sample preparation times which probably resulted in different humidity content of the fibres in capillaries. The shortest and the longer preparation times are represented in figure 1a and figures 1b-c, respectively. The patterns are quite reproducible for a given sample. In addition, no difference between frozen and fresh samples was observed. The zone corresponds to the scattering vector range from 0.005 $Å^{-1}$ to 0.16 $Å^{-1}$ along the equator (horizontal) and from 0.005 $Å^{-1}$ to 0.055 $Å^{-1}$ along the meridian. Each pattern is in fact an average of five consecutive patterns collected along a transverse scan after background subtraction.

The patterns are clearly anisotropic. The series of sharp reflections in the SAXS region along the meridian correspond to the various orders of the long-range period (about 650 Å).

The other major scattering component appears along the equator. It consists of an intense and broad reflection located around 0.08 $Å^{-1}$, *i.e.* 12.5 Å in real space. No sharp Bragg reflection is visible, which proves the lack of lateral long-range crystalline order. The shape and the position of the reflection are slightly different on the three patterns. Differences in the axial extent of this reflection simply reflects a greater or lesser dispersion of the molecules axes orientation (low dispersion in figure 1c and higher dispersion in figure 1a). The difference in radial position and shape will be discussed hereafter. Another difference lies in the more or less intense diffuse and broad butterfly-like streak which extends from the center of the pattern up to the broad reflection. It is hardly visible in figure 1a whilst being intense in figure 1c. The set of our patterns clearly indicates a correlation between the intensity of this streak and the position of the broad reflection; the more intense is it, closer to the origin the reflection is.

Our objective is to model the whole equatorial intensity profile, composed of the main reflection and the butterfly-like streak, using the paracrystal modelling, and secondly to test the sensitivity of this modelling by looking at the pattern modifications arising from different preparation times.

3.2 Modelling the lateral packing of collagen triple helices

The modelling method was tested on the equatorial intensity profile of the highest hydration grade pattern (figure 1a). The set of collagen triple helices is treated as full and infinite cylinders located at the nodes of a two-dimensional paracrystal-type distorted hexagonal lattice. Three parameters are implemented in this model: the diameter of the cylinders (ϕ), the average hexagonal unit cell length (a) and the standard deviation of the distribution of this length (σ) (in percentage of the unit cell length), which provides a measure of the degree of disorder. The first two parameters were found in literature as in the crystal structure of a collagen-like peptide at 1.9 Å resolution [12]. Looking down the helical axis, the molecules of ~ 10 Å in diameter are located at the nodes of a quasi-hexagonal lattice with a unit cell length (a) of 14.0 Å. Since there is no data in the literature on the degree of disorder, this parameter will be deduced from our modelling.

Figure 2 shows the comparison between the experimental profile and the modelled one choosing: ϕ = 10.8 Å, a = 13.3 Å and σ = 15%. The profiles are similar for the main peak but the fitting is less good outside. This can be explained by the fact that the paracrystal modelling generally overestimates the scattered intensity at low angles.

The two terms $|F_{mf}(S)|^2$ and Z(S) are also represented to visualize their relative contribution. The value of Fourier transform of the cylinders $|F_m(S)|^2$ decreases continuously down to $S=1/\phi$ Å^{-1} and it remains low for larger S values. Away from the origin, the interference function Z(S) presents a first peak at a S value which is close to the theoretical value for a perfect hexagonal lattice: $S = 2/a\sqrt{3}$ Å^{-1} (0.0868 Å^{-1}). Interestingly, because of the negative slope of $|F_m(S)|^2$, the peak position in the modelled intensity profile is shifted towards smaller S values. In our case the total shift is small (2.7%), however it can sometimes be quite larger. This effect therefore must to be taken into account for a correct determination of the hexagonal lattice unit cell length. Consequently, the best modelling strategy for collagen consists of estimating first the σ value from the width of the experimental peak and subsequently derive the best values of a and ϕ.

It can be seen in figure 2 that the intensity profile is mainly determined by the first order peak of Z(S), both in position and width. At higher scattering angles, Z(S) presents a series of weaker and broader maxima. Their intensity decreases when the degree of disorder σ increases whilst their width, especially for the first peak, strongly increases.

3.3 Sensitivity of the modelling relative to parameters

The present analysis clearly indicates that the use of the hexagonal paracrystal concept leads to a reasonably good fitting of the broad scattering peak arising from the non-perfect lateral packing of the collagen triple helices in a tissue, as it does for keratin intermediate filaments.

The sensitivity of the simulation was tested by introducing slight changes in the three parameters ϕ, a and σ. The resulting effect is illustrated in figure 3.

A change of 0.8 Å in ϕ (the molecular diameter) does not lead to any significant change in the modelled profile. This is due to the term $|F_m(S)|^2$ which is not very sensitive to molecules diameter. On the contrary, slight changes in a and σ lead to significantly different modelled profiles. An increase in a by 0.9 Å (from 13.3 to 14.2 Å, i.e. 7%) shifts the position of the maximum of the reflection from 0.0868 down to 0.0770 Å^{-1}, *i.e.* by 11%. Similarly, increasing the degree of disorder σ from 15 to 20% not only broadens significantly the peak but also shifts its position down to 0.0804 Å^{-1}, i.e. by 7%.

The modelling procedure is therefore quite sensitive both to the degree of disorder and to the unit cell length (typically a 2% shift is detectable), but is not very sensitive to the diameter of the molecules.

3.4 Sensitivity of the modelling versus changes in collagen packing

The scope of our modelling method has been tested by comparing the results obtained for pattern 1a with those of patterns 1b and 1c. Resulting from different preparation times, the water content for samples corresponding to patterns 1b and 1c was lower than for pattern 1a. The comparison between the experimental profiles and the modelled ones is shown in figure 4. The conclusion is straightforward: the change in both position and width of the intensity profiles essentially corresponds to a huge change of the disorder grade σ, respectively 15%, 22.5% and 32.5%, from the most hydrated sample (figure 1a) to the less hydrated one (figure 1c); it is not due to changes in the length of the unit cell; the slight increase in *a* for modellings of 1b and 1c (13.6 Å instead of 13.3 Å for 1a) only plays a minor role in the result. Considering only the shift in peak position without taking into account its profile change would have led to the erroneous conclusion of an increase of *a* from 13.74 Å up to 16.01 Å!
Our analytical modelling method based on the paracrystal concept is therefore well adapted to explain slight changes in the structure of the non-perfect lateral hexagonal packing inside collagen fibrils.

4. Discussion - Conclusions

Spectacular results in the understanding of the lateral structure of the collagen triple helices inside the fibre have been recently deduced from X-ray diffraction experiments carried out on highly crystallised fibres which are generally obtained by immersing the freshly extracted fibres into a salt-controled medium [3]. The packing model can be described by a complex combination of square and triangular unit sets of triple helices. In comparison, our scattering patterns of freshly extracted and untreated fibres do not exhibit any series of equatorial reflections, indicating a poorly defined lateral order. The question of the nature of this order is important not only for the characterization of untreated collagen fibres but also because, even in a controled environment, part of the structure remains non crystallized. To our knowledge, few studies have analysed and modelled the lateral packing of collagen triple helices when this structure is disordered. The concept of using short range order to explain the X-ray

equatorial scattering from collagen also reproduces correctly the experimental profile [6] but it does not contain any echo of a hexagonal order, and thus is not informative about the actual structural characteristics. The paracrystal approach is therefore interesting since it is based on a disordered hexagonal lattice; in this way, the average hexagonal order is retained whatever the degree of disorder is. In addition modelling with the paracrystal concept is simple and analytical. The present work showed a good agreement with experimental profiles concerning the peak profile, its position and the diffuse streak down to the origin. This modelling method is quite sensitive to the degree of disorder and to the average inter-object distance.

One of the clearest and unexpected data which is highlighted by our modelling using the paracrystal concept is that the shift of peak positions can arise from a change in the degree of order without any change of the distance between objects. This underlines the importance of evaluating the degree of order before attributing a shift in peak position to a change in the unit cell. As it is difficult to estimate and to model, the degree of order is not sufficiently taken into account in the characterisation of poorly ordered structures. The paracrystal-based modelling enables to measure and to follow it. The way to differentiate a peak position shift due to a change in inter-object distance from a shift due to a change in the degree of order is to look first at the peak width. If the width is the same, then it is a pure change of distance, otherwise the shift is at least partly due to a change of the degree of disorder. In addition, an increase of disorder leads to a more intense diffuse streak along the equator.

In terms of interpretation, changes in a given structure, from an ideal to a less ordered one indicates a higher variability of the distances between objects, i.e. to a greater dispersion of interactions between objects. These interactions are generally weak polyelectrolyte-type interactions in the case of organic fibres, so they are likely to change easily. Most techniques only give information on the average of the interaction, the paracrystal modelling gives in addition the dispersion. This dispersion may provide important indications on the behavior of fibre assemblies and their deformability.

The X-ray equatorial scattering method based on the paracrystal concept had been used successfully for keratin. The present study tends to indicate that it is also appropriate to model collagen scattering patterns. Moreover, there is every reason to believe that this method it is

well suited for modelling all molecules involved in fibrillar imperfect hexagonal networks, as for example the columnar phase of DNA .

Figure Captions

Figure 1

X-ray microdiffraction patterns of single mouse tail fibres in the scattering vector range 0.005 $Å^{-1}$ to 0.16 $Å^{-1}$ along the equator (horizontal) and 0.005 $Å^{-1}$ to 0.055 $Å^{-1}$ along the meridian (vertical) recorded at the ESRF beamline ID13. The fibres are placed vertically. Figure 1a and 1c correspond to the shortest and longest preparation times, respectively and probably leading to different hydration grades. The main differences concern the position of the equatorial broad reflection and the diffuse butterfly-like streak which extends from the center of the pattern up to the broad reflection (it is clearly visible in figure 1c whilst hardly visible in figure 1a).

Figure 2

Principle of the X-ray scattering modelling in the equatorial reciprocal plane showing the two various intensity components:

- the square modulus of the Fourier transform of the projection of the electronic density for the molecule onto the equatorial plane, which is supposed to be disk-shaped and uniform (diameter ϕ),
- the interference function Z(S) for the hexagonal paracrystal model witch only depends on the unit cell length (a) and on its standard deviation (σ).

The modelled profile which is equal to the product of these two components is compared to the experimental profile of figure 1a.

Figure 3

Various equatorial intensity profiles showing the sensitivity of the modelling *versus* the three parameters: the molecular diameter (ϕ), the unit cell length (a), and its standard deviation (σ). The modelled profiles are quite sensitive to the parameters (a) and (σ), whilst poorly sensitive to ϕ. The experimental profile is the one of figure 1a.

Figure 4

Comparison of modelled and experimental equatorial patterns for figures 1a, 1b and 1c.
Variations of σ values show well reproduced intensity profiles The changes in the intensity profiles are well reproduced only. This means that the structural change concerns the disorder

grade, and not the distance between molecules as could be errouneously suggested by the change of the peak position.

References

[1] G. Mosser, A. Anglo, C. Helary, Y. Bouligand, M.-M. Giraud-Guille, Dense tissue-like collagen matrices formed in cell-free conditions, Matrix Biology 25 (2006) 3 – 13.

[2] B. Pansu, E. Dubois-Violette, Blue phases : experimental survey and geometrical approach,
J. Phys. Colloques 51 (1990) C7-281-C7-296.

[3] T. J. Wess, A. P. Hammersley, L. Wess, A. Miller, Molecular Packing of Type I Collagen in Tendon, J. Mol. Biol. 275 (1998) 255-267.

[4] J. F. Sadoc, R. Mosseri, Geometrical Frustration, Cambridge University Press, 1999.

[5] J.K. Percus, G.J. Yecick, Analysis of Classical Statistical Mechanics by Means of Collective Coordinate, Phys. Rev. 110 (1958) 1-13.

[6] J.Woodhead-Galway, P. A. Machin, Modern theories of liquids and the diffuse equatorial X-ray scattering from collagen, Acta Cryst. A32 (1976) 368-372.

[7] F. Briki, B. Busson, J. Doucet, Organization of microfibrils in keratin fibers studied by X-ray scattering modelling using the paracrystal concept, Biochem Biophys Acta: 1429 (1998) 57-68.

[8] R. Hoseman, Der ideale Parakristall und die von ihm kohiirente Röntgenstrahlung., Z. Physik 128 (1950) 465-492.

[9] B. Busson, J. Doucet, Distribution and interference functions for two-dimensional hexagonal paracrystals, Acta Cryst.A (2000) A56, 68-72.

[10] J. P. R. O. Orgel, T.C. Irving, A. Miller, and T.J. Wess, Microfibrillar structure of type I collagen in situ, PNAS 103 (2006) 9001–9005.

[11] C. Riekel, M. Burghammer, M. Müller, Microbeam small-angle scattering experiments and their combination with microdiffraction. J. Appl. Cryst. 33 (2000) 421-423.

[12] J. Bella, M. Eaton, B. Brodsky, H.M. Berman, Science, Crystal and molecular structure of a collagen-like peptide at 1.9 Å resolution 266 (1994) 75-81.

Figure 1

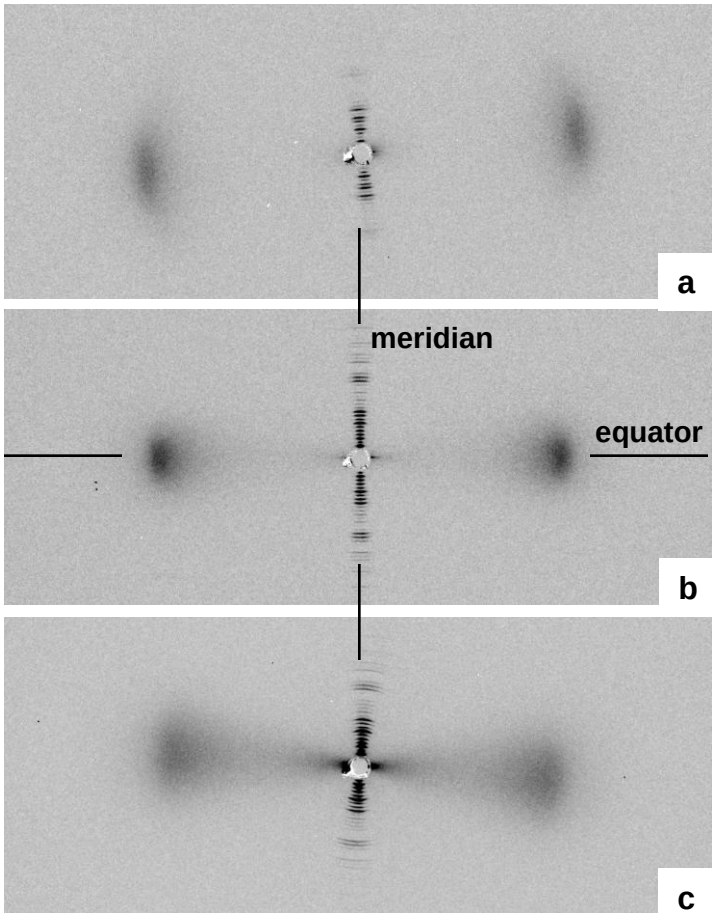

Figure 2

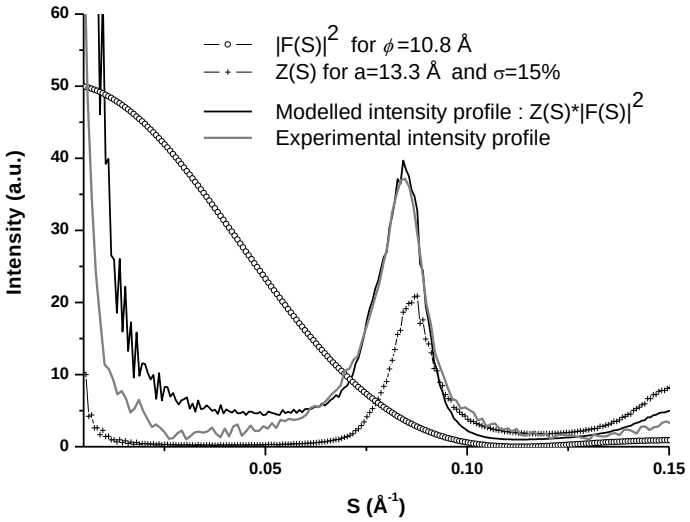
|F(S)|2 for ϕ=10.8 Å
Z(S) for a=13.3 Å and σ=15%
Modelled intensity profile : Z(S)*|F(S)|2
Experimental intensity profile
Intensity (a.u.)
S (Å-1)
0
10
20
30
40
50
60
0.05
0.10
0.15

Figure 3

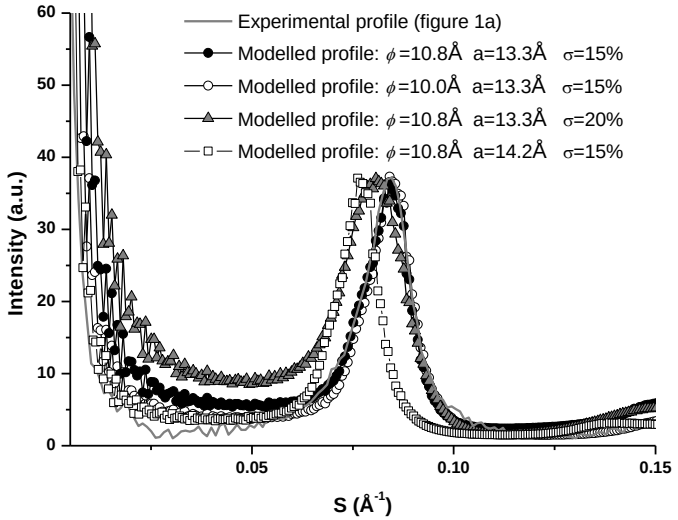
Experimental profile (figure 1a)
Modelled profile: ϕ=10.8Å a=13.3Å σ=15%
Modelled profile: ϕ=10.0Å a=13.3Å σ=15%
Modelled profile: ϕ=10.8Å a=13.3Å σ=20%
Modelled profile: ϕ=10.8Å a=14.2Å σ=15%
Intensity (a.u.)
S (Å-1)
0
10
20
30
40
50
60
0.05
0.10
0.15

Figure 4

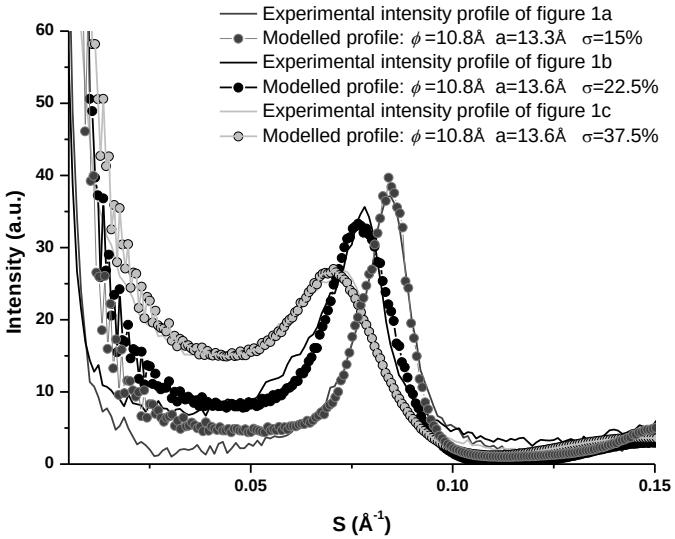
Experimental intensity profile of figure 1a
Modelled profile: ϕ=10.8Å a=13.3Å σ=15%
Experimental intensity profile of figure 1b
Modelled profile: ϕ=10.8Å a=13.6Å σ=22.5%
Experimental intensity profile of figure 1c
Modelled profile: ϕ=10.8Å a=13.6Å σ=37.5%
Intensity (a.u.)
S (Å-1)
0
10
20
30
40
50
60
0.05
0.10
0.15